

# Thermal Performance of the Urban Weather Generator Model as a Tool for Planning Sustainable Urban Development

Noelia Liliana Alchapar<sup>A</sup>, Cláudia Cotrim Pezzuto<sup>B</sup>, Erica Norma Correa<sup>A</sup>, Agnese Salvati<sup>C</sup>

Received: November 30, 2019 | Revised: December 28, 2019 | Accepted: December 30, 2019

DOI: 10.5937/gp23-24254

## Abstract

The research aims at assessing the sensitivity of the Urban Weather Generator v4.1 to the application of different mitigation strategies for the urban heat island under two climatic contexts: desert climate (Mendoza city) and tropical climate (Campinas city). Twenty-four scenarios that modify their morphologic and material parameters were simulated. The results showed that the temperature of the air predicted by the UWG model is not significantly sensitive to the changes produced by the application of different strategies in urban contexts of equal H/W aspect; however, it does show sensitivity to the variation of the H/W aspect ( $\Delta T_a \leq 1.3^\circ\text{C}$ ) and the climate context. The highest performance of the UWG model was recorded on the surface temperatures of the urban envelope, with a maximum difference in surface temperature was recorded on high aspect ratio with high albedo in arid climate, ( $T_s$  of roof =  $28^\circ\text{C}$ ).

**Keywords:** Thermal performance; strategies; H/W; high albedo; Urban Weather; city

## Introduction

The phenomenon of the Urban Heat Island (UHI) has energy, environmental and social consequences, deteriorating the quality of life of the citizens. Understanding its magnitude and its characteristics is a prerequisite for urban planning aimed at mitigating and adapting to climate change. Studies related to urban climate report that the increase in urban temperature is directly attributed to anthropic actions and that temperature rise aggravates energy consumption for refrigeration, it increases peak electricity demand, intensifies pollution problems, causes human discomfort and health problems such as heat-related illnesses and premature deaths in cities (Doyon et al., 2008; Mirzaei & Haghighat, 2010). Strategies to mitigate urban warming are based on two basic principles: to increase the vegetation cover of urban

spaces (Bowler et al., 2010; Chang & Li, 2014; Perini & Magliocco, 2014) and to encourage the best thermal and optical performance of urban surface materials.

In terms of mitigation strategies for urban warming, several methodologies have been applied to predict and mitigate the effects of this phenomenon. Recently, the use of computing technology has been intensified due to the limitations of observational methods. Therefore, before implementing the results in the process of urban planning, it is necessary to evaluate the calibration of climate models and their predictive capacity, and the to what extent to which simulation models are capable of representing real situations, before implementing the results in the process of urban planning (Mao et al., 2018).

<sup>A</sup> Institute of Environment, Habitat and Energy (INAHE), CONICET, Argentina

<sup>B</sup> Urban Infrastructure Graduation Program, Pontifical Catholic University of Campinas, Brasil

<sup>C</sup> Brunel University London, UK

\* Corresponding author:

In addition to observational approaches, mathematical models have been developed to solve urban climate problems, including UHI. Among these models, the Energy Balance Model (EBM) and the Computational Fluid Dynamics -CFD models- were the most reliable and presented satisfactory results. There are 4 types of models for urban climate analysis: mesoscale weather models, microclimate models, energy building models, and human thermal models (Ooka, 2007; Sola & Corchero et al., 2018).

ENVI-met (Bruse & Fleer, 1998) is the most relevant microclimatic scale computer scale model, based on the CFD models which includes parameters of short wave and long wave radiation, transpiration, evaporation and sensible heat flux from vegetation, water, and soil. In a new version, ENVI-met 4.0 has implemented a 3D vegetation model that allows the description of various plant shapes and special distribution of trees, resulting in a greater adjustment in the percentage of sky view factor (SVF) in the urban canyon. It also introduces equations that consider the thermal inertness of the wall and roof (Acero et al., 2015; Yang et al., 2013). In recent studies, we have demonstrated ENVI-met's prediction ability to reproduce urban temperatures with different scenarios by applying UHI mitigation strategies in Latin American cities (Alchapar et al., 2017). This work demonstrates that the scenarios that reach lower air temperatures have the highest percentage of urban vegetation and high levels of albedo in the road and roof surfaces.

As an alternative to mesoscale computing models, Bueno et al. (2013b) proposed the Urban Weather Generator (UWG) designed to estimate air temperature in the Urban Canopy Layer (UCL) using weather information collected by an operational weather station. The UWG model consists of four calculation components: Rural Station Model, Vertical Diffusion Model, Urban Boundary-layer (UBL) model and Urban Canopy and Building Energy Model (Bueno et al., 2015). The UWG model is based on the Town Energy Balance (TEB) scheme, and on the Building Energy Model, taking into account the reciprocal interactions between urban area characteristics and rural weather data (Masson, 2000). The UWG can also estimate the energy relationship between buildings and the urban climate because the energetic model derives from EnergyPlus algorithms. In the new version of UWG model the solar radiation and the calculation of the infrared radiation have been upgraded. It is also possible to add a user-defined routine for traffic-generated heat flow using the EPW file on soil temperature to obtain the boundary condition values to get the layer temperature profile (Mao et al., 2017).

Recent research has used the UWG in data from Basel (Switzerland), Toulouse (France) and Singa-

pore, showing an average error of about 1K (Bueno et al., 2013a; Bueno et al., 2014). The model calculates the hourly air temperature in the urban canyon according to a parametric description of the urban area (Salvati et al., 2019). This compared the UWG model predictions with real observations at different urban sites in Rome and Barcelona. The results showed that the UWG model can capture the general temperature trend of a city, especially in homogeneous urban contexts.

In the present work we investigated the thermal performance of the results obtained by the Urban Weather Generator (UWG v4.1) proposed by (Bueno et al., 2013a; Bueno et al., 2013b), which estimates the air temperature in the urban canopy layer (UCL) by using weather data and input data of urban characteristics. This paper was carried out under two climatic contexts in two Latin American cities: Mendoza, Argentina and Campinas, Brazil (Figure 1). The average Urban Heat Island (UHI) of Mendoza is 6.5°C, with maximum peaks of 10°C during the night period, as a result of the morphological characteristics of the city, the intense afforestation of urban canyons and the urban surface materials (Cor-

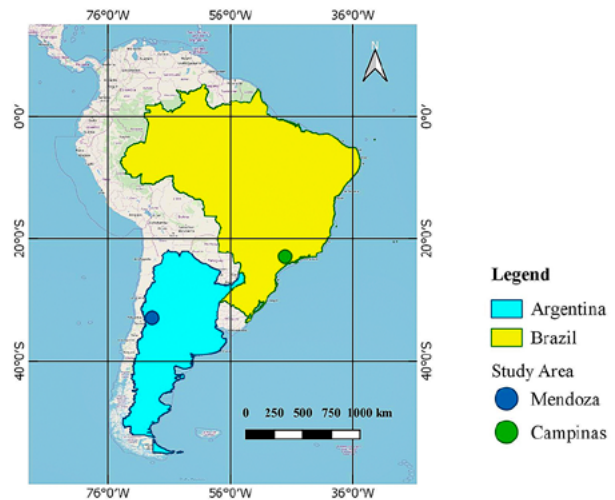


Figure 1. Location map for Mendoza city (Argentina) and Campinas city (Brazil)

rea, 2006). In the city of Campinas the Urban Heat Island (UHI) reaches maximum values of 6 °C (Pezzuto, 2007). According to Köppen–Geiger climate classification system (Kottek et al., 2006), Mendoza, Argentina is classified as desert climate with cold steppe/desert category (BWk), and Campinas, Brasil, is placed in the category of warm temperate climate with dry winters and hot summers (Cwa). Twenty-four different scenarios have been analyzed that modify their percentage of vegetation; albedo level of envelope materials and building's aspect ratio (H/W) have been analyzed.

## Methodology

### Characteristics of the analyzed cities

The cities of Mendoza and Campinas were selected as areas of study to quantify the predictive capacity of the UWG by modifying morphological and material parameters.

In Table 1, the main characteristics of each city are described (Mendoza Aero Observations, 2019 and CEPAGRI / UNICAMP, 2019). It should be noted that be-

tween both cities there is an approximate difference in latitude of 10 °C (Mendoza: 32.54 °and Campinas: 22.53°C). This distance to the Equator impacts directly on the solar height and consequently on the intensity of solar radiation.

Figure 2 shows the annual global horizontal radiation distribution obtained from the climatic EPW archives (Climate.Onebuilding.Org, 2019).

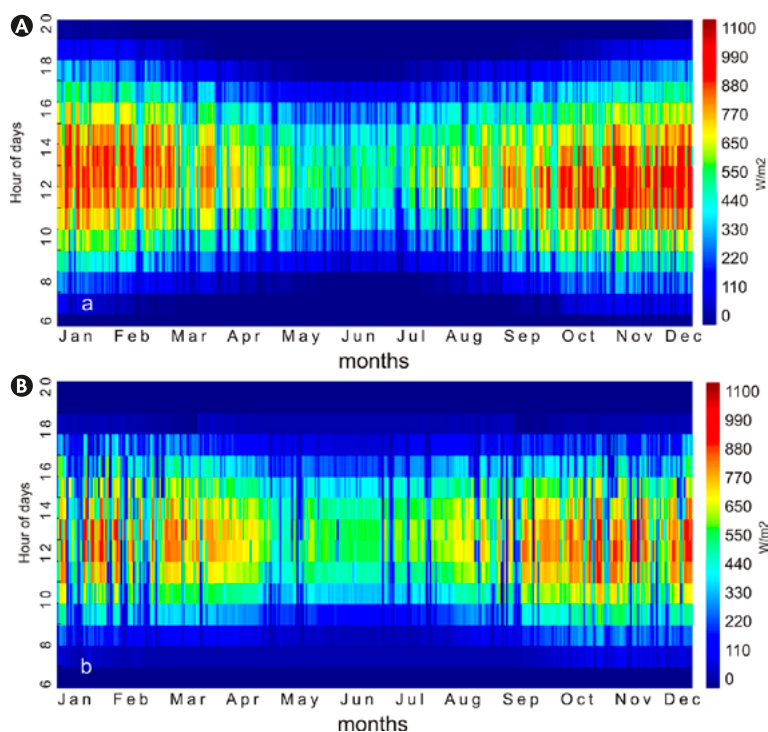


**Figure 2.** Annual horizontal global radiation mapping ( $W/m^2$ ). Mendoza city (A) and Campinas (B).

Source: Elaborated by the author, 2019

**Table 1.** Geographical and climatic conditions of the cities evaluated.

Features	Mendoza City	Campinas City
Location	32°54'48"S, 68°50'46"W; 750m a.s.l.	22°53'20"S, 47°04'40"W; 680m a.s.l..
Territorial area	368 km <sup>2</sup>	794 km <sup>2</sup>
Population	1, 089,000 inhabitants	1,194,094 inhabitants
Climate according to Köppen classification (Kottek et al., 2006)	Desert with cold steppe ( <i>BWk</i> )	Warm temperate with dry winters and hot summers ( <i>Cwa</i> )
Climate Zone ASHRAE,2006	2B Warm dry	2A Warm wet
Annual precipitations	218mm	1372 mm.
Annual maximum daily solar radiation	1006 $W/m^2$	814 $W/m^2$
Maximum daily summer solar radiation	1089 $W/m^2$	961 $W/m^2$
Wind speed at 10m	1.9m/s (southeast)	2.2 m/s (southeast)
Average annual temperature	16.50 °C	21.40°C,
Average maximum temperature	24.50 °C	27.10 °C
Average minimum temperature	9.60 °C	15.60 °C

Source: Elaborated by the author, 2019

### Study area description

As a case study, a frequent social neighborhood typology of Latin American cities was selected. The studied area is situated in the district of Las Heras, Mendoza, Argentina. The average building height is 3.2 m, with aspect ratio (H/W) that ranges between 0.15 and 0.19. The Street width ranges from 16 to 20 m and the sidewalk is 3 m. The species *Morus alba* blanco is the predominant urban afforestation (Sosa, Cantaloube, & Canton, 2017).

The facades of the buildings register an average albedo ( $\hat{\alpha}$ ) of 0.25. The roofs are predominantly covered with Terracotta ceramic tile ( $\hat{\alpha} = 0.35$ ) The pave-

ment and sidewalks are composed of different types of calcareous stones ( $\hat{\alpha} = 0.30$ ), and the vehicular pavement is made of concrete ( $\hat{\alpha}=0.25$ ) (Alchapar & Correa, 2016). The study was conducted during the summer period because of the extreme weather conditions (Figure 3).

### Scenarios evaluated

24 scenarios were simulated considering three aspects: percentage of vegetation (current and without vegetation); albedo level of envelope materials and aspect ratio H/W. Table 1 outlines the characteristics of each scenario (Table 2).



Figure 3. Aerial image of the study area and within the urban canopy.  
Source: Adapted Google Earth (2019)

Table 2. Morphological and material characteristics of proposed scenarios

Low H/W (0.16)					
Vegetated		Cod.	No Vegetation		Cod.
$\hat{\alpha}$ low	roof: 0.20	L1.a	$\hat{\alpha}$ low	roof: 0.20	L1.b
	road: 0.20			road: 0.20	
	wall: 0.20			wall: 0.20	
$\hat{\alpha}$ high	roof: 0.80	L2.a	$\hat{\alpha}$ high	roof: 0.80	L2.b
	road: 0.75			road: 0.75	
	wall: 0.80			wall: 0.80	
$\hat{\alpha}$ combined	roof: 0.80	L3.a	$\hat{\alpha}$ combined	roof: 0.80	L3.b
	road: 0.75			road: 0.75	
	wall: 0.20			wall: 0.20	
High H/W (1.8)					
Vegetated		Cod.	No Vegetation		Cod.
$\hat{\alpha}$ low	roof: 0.20	H1.a	$\hat{\alpha}$ low	roof: 0.20	H1.b
	road: 0.20			road: 0.20	
	wall: 0.20			wall: 0.20	
$\hat{\alpha}$ high	roof: 0.80	H2.a	$\hat{\alpha}$ high	roof: 0.80	H2.b
	road: 0.75			road: 0.75	
	wall: 0.80			walls: 0.80	
$\hat{\alpha}$ combined	roof: 0.80	H3.a	$\hat{\alpha}$ combined	roof: 0.80	H3.b
	road: 0.75			road: 0.75	
	wall: 0.20			wall: 0.20	

Source: Elaborated by author, 2019.

### Micro-climatic data and input parameters

The UWG simulation requires two input data: rural weather data provided in the EPW format and input data of urban characteristics inserted from the MATLAB program with XML and Excel interfaces (Bueno et al., 2013a; Mao et al., 2017). The urban characteristics of the study area include: microclimate parameters, urban building characteristics, vegetation parameters, building types and simulation parameters. The micro-climatic parameters define the characteristics of the Urban Boundary Layer of the referential cities (Mendoza and Campinas in this study). Urban parameters include morphological and material factors such as urban geometry (average building height, building density, vertical to horizontal ratio), albedo level of materials (street, facades, and roofs) and sensible and latent anthropogenic heat. The vegetation parameters include urban area vegetation/tree coverage and the vegetation albedo. The percentage parameters in the reference area of different types of buildings (apartment, primary

school, large office, supermarket, warehouse, etc.) are defined in the typology of buildings. The main input parameters are presented in Table 3.

**Table 3.** UWG simulator input parameters.

Urban characteristics	Low H/ W= 0.16	High H/ W= 1.8
Building average height(meters)	3.2	30
Vertical proportion to the horizontal	0.3	6.13
Urban Area Veg Coverage (%)	26	26
Urban Area Tree Coverage (%)	23	23
Anthropogenic sensitive heat (W/m <sup>2</sup> ) *	4.5	20
<b>Albedo enveloped</b>		
Roof	0.20 - 0.80	
Road	0.20 - 0.75	
Wall	0.20 - 0.80	

\* Data: Correa, 2006

Source: Elaborated by author, 2019.

## Results

### Thermal performance of the UWG simulator according to scenarios

#### Air temperatures within Urban Canopy Layer (Ta\_UCL)

Figure 4 shows the air temperature curves of the urban canopy (Ta\_UCL) of the total proposed scenarios, in relation to rural temperature (Ta\_rural).

After simulating the 24 scenarios proposed in both cities, there are no significant changes in the Ta\_UCL.

In both cities, the UWG model does not show sensitivity to the increased albedo levels of envelope or to the modification of the vegetation percentage ( $\Delta Ta_{UCL}$  between scenarios  $\leq 0.5$  °C for both cities). The modification of behaviors in the Ta\_UCL becomes evident only when the H/W aspect rises, mainly during the cooling period, with  $\Delta Ta_{UCL}$  between scenarios  $\leq 1.3$  °C for both cities. These results confirm the main role of geometric parameters in the calculation of the UWG, which was highlighted in previous stud-

**Table 4.** Air temperature: maximum (max), minimum (min), media (med)-, records in the reference station (Ta rural) and in urban canopy (Ta\_UCL) of 24 scenarios.

Air Temperature °C	Scenarios	Mendoza City			Campinas City		
		Max	Min	Med	Max	Min	Med
Ta rural	38	10	25.1	32.4	12.5	21.8	
Ta_UCL	L1.a	38	12.3	26.9	32.4	13.9	23
	L1.b	37.9	12.3	26.9	32.5	13.8	23
	L2.a	37.5	12.3	26.7	32	13.9	22.8
	L2.b	37.5	12.2	26.5	31.9	13.9	22.7
	L3.a	37.5	12.3	26.7	32	13.9	22.8
	L3.b	37.5	12.2	26.5	31.9	13.9	22.7
	H1.a	38.9	13.9	28	32.5	15.1	24
	H1.b	38.9	13.9	28	32.5	15.1	24
	H2.a	38.7	14	28.1	32.7	15.1	24
	H2.b	38.7	14	28.1	32.6	15.1	24
	H3.a	38.7	14	28.1	32.7	15.1	24
	H3.b	38.7	14	28.1	32.6	15.1	24

Source: Elaborated by the author, 2019

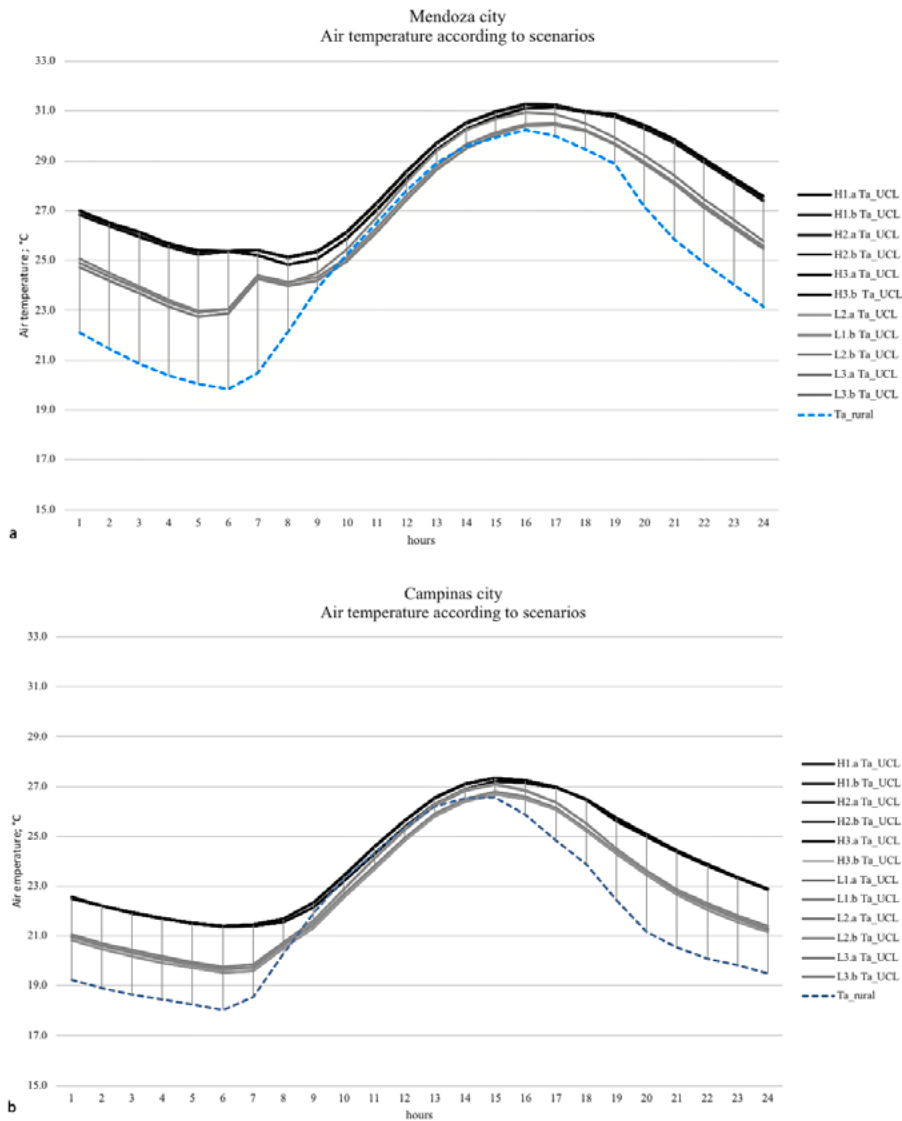


**Figure 4.** Air temperature curves of Mendoza scenarios ( $T_{a\_UCL}$ ) according to albedo level percentage of vegetation and H/W. a. Mendoza city. b. Campinas city.

Source: Elaborated by the author, 2019

ies in cities of the Mediterranean and South America (Palme et al., 2018; Palme et al., 2016; Salvati et al., 2019; Salvati et al., 2017). According to simulated data, in Mendoza, the UHI in high H/W reaches 5.4 °C and in low H/W 2.7 °C in Mendoza, while in Campinas, the UHI is 3.4 C in high H/W and 1.5 °C in low H/W. In other words, the magnitude of the impact of the presence of the city over air temperature is greater in Mendoza city (Table 4).

#### Surface temperatures of enveloped ( $T_s$ )

To evaluate the sensitivity of the numerical model on the surface temperature ( $T_s$ ) of the urban envelope, the analysis was organized according to the following three parameters:

**H/W aspect:** Low= 0.16 (L) and High= 1.8 (H)

- **Mendoza:** When comparing the surface thermal performance of the envelope elements, it is observed

that, with high H/W due to the effect of the shadows cast by the buildings, the  $T_{s\_road}$  and  $T_{s\_wall}$  are smaller than with low H/W. It recorded maximum temperature differences equal to  $\Delta T_{s\_road} \leq 11.9$  °C and  $\Delta T_{s\_wall} \leq 3.4$  °C between scenarios with identical vegetal and material configurations were recorded (see H1.b vs. L1.b in Table 5 and Fig.5.a).

- **Campinas:** The same trend occurs in the city of Campinas, a scenario with higher H/W wich records lesser surface temperatures of roads and walls.  $\Delta T_{s\_road} \leq 7$  °C, (see H1.b = 35 °C vs. L1.b = 42 °C) and  $\Delta T_{s\_wall} \leq 3.4$  °C (see H1.b = 31.4 °C vs. L1.b = 38.4 °C in Table 5 and Fig.5.b).

These results suggest that, for the summer period, the impact of the modification of H/W aspect is greater in Mendoza than in Campinas, due to high heliophany and low wind speed.

**Albedo level:** 1= low albedo; 2= high albedo;3= combined albedo

- **Mendoza:** By contrasting the scenarios that modify albedo levels and keeping the rest of the parameters the same, a great impact on roof temperatures was observed. Scenarios with low albedo levels (1) further increase their surface temperatures in the total envelope. The resulting differences are:  $\Delta T_{s\_road} \leq 6.2$  (L1.a=43.6°C vs. L2.a/L3.a=37.4°C);  $\Delta T_{s\_wall} \leq 4.1$  (L1.a=41.2°C vs. L2.a/L3.a=37.1°C in Table 5 y Fig.4.a);  $\Delta T_{s\_roof} \leq 13^\circ\text{C}$  in low H/W and until  $28^\circ\text{C}$  in high H/W (L1.a=53.8°C vs. L2.a/L3.a=40.5°C and H1.a=70.5°C vs. H2.a/H3.a=42.6°C in Table 5 y Fig.5.a).

- **Campinas:** As in Mendoza, the higher surface temperatures are recorded in scenarios with low albedo levels (1). The resulting differences are:  $\Delta T_{s\_road} \leq 5.5^\circ\text{C}$  (L1.a=37.1°C vs. L2.a/L3.a=31.6°C);  $\Delta T_{s\_wall} \leq 3.5$  (L1.a=34.7°C vs. L2.a/L3.a=31.2°C);  $\Delta T_{s\_roof} 12.9 \leq ^\circ\text{C}$  in low H/w and until  $24.3^\circ\text{C}$  in high H/W aspect (L1.a=47.1°C vs. L2.a/L3.a=34.2°C y H1.a=61.1°C vs. H2.a/H3.a=36.8°C in Table 5 y Fig.5.b).

The UWG model shows the following behavior patterns in both cities. The scenarios with high albedo (2) and combined (3) levels have identical behaviors. This means that the numerical model does not show sensitivity in this aspect. In addition, the modification of

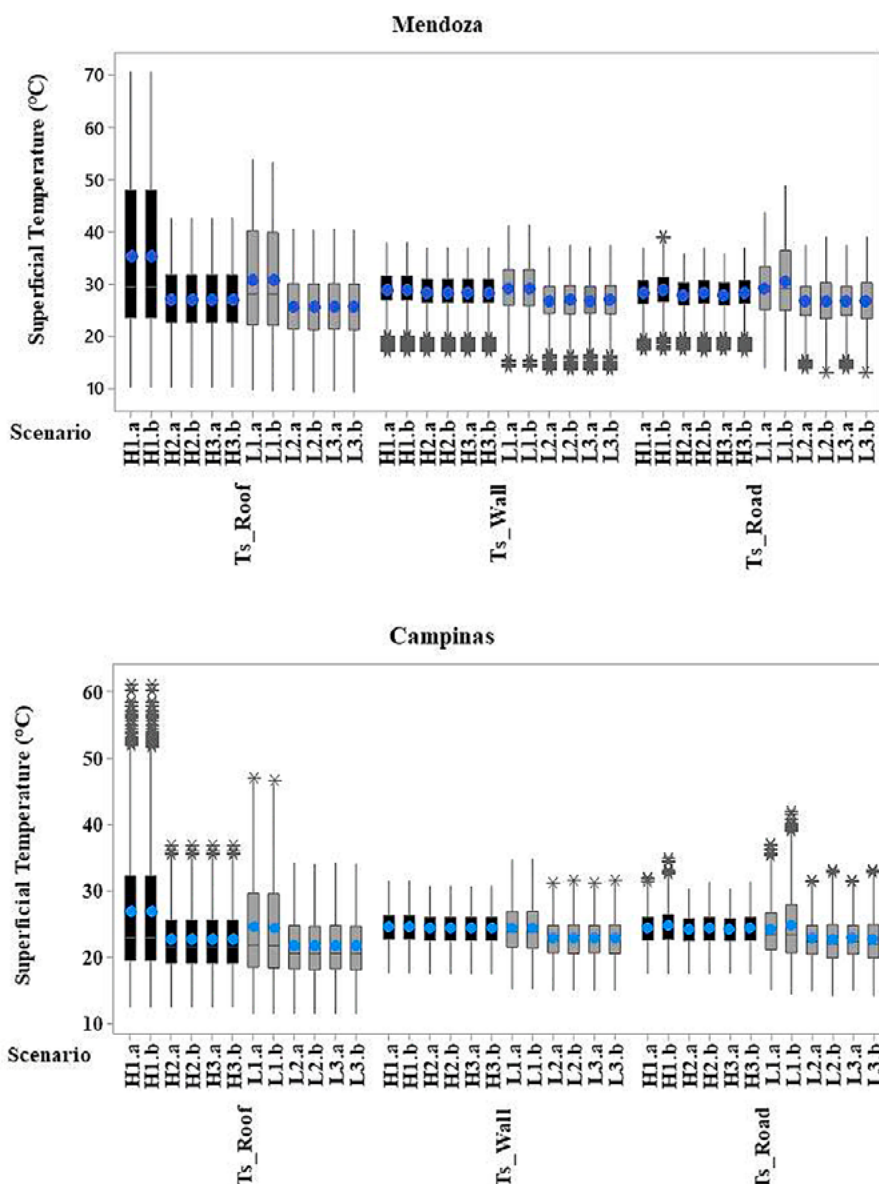


**Figure 5.** Box plot diagram of surface temperatures in the both cities studied. Black columns indicate high H/W scenarios and gray columns indicate low H/W scenarios. a. Mendoza city. b. Campinas city.

Source: Elaborated by the author, 2019.

albedo levels has a greater impact on surface temperatures – first in high H/W aspect -, second, on walls and finally on roads with low H/W scenarios.

Finally, when the levels of albedo were modified, the two cities show the same tendency to decrease surface temperatures; however, the impact potential is greater in Mendoza due to the high solar radiation during the summer period.

**Vegetation presence:** a = with vegetation; b = without vegetation

- In both cities the presence of urban green modifies the thermal performance of road surfaces ( $\Delta T_{s\_calles} \leq 5^{\circ}C$ ) in low H/W scenarios with low albedo level (L1.a vs L1.b in Mendoza and Campinas in Table 6). This is due to the fact that the vegetation percentage is relatively low (23 and 26% respectively) in the evalu-

**Table 5.** Surface temperatures: maximum (max), minimum (min), average (med) of 24 scenarios. According to enveloped type: roofs (Ts\_roof), vehicular and pedestrian circulations (Ts\_road) and facades (Ts\_wall)

Surface temperature °C		Mendoza City			Surface temperature °C		Campinas City		
		Max	Min	Med			Max	Min	Med
L1.a	Ts_roof	53.8	9.8	30.8	L1.a	Ts_roof	47.1	11.5	24.5
	Ts_road	43.6	14	29.2		Ts_road	37.1	15	24.2
	Ts_wall	41.2	14	29.2		Ts_wall	34.7	15.2	24.3
L1.b	Ts_roof	53.3	9.6	30.6	L1.b	Ts_roof	46.7	11.4	24.4
	Ts_road	48.8	13.5	30.6		Ts_road	42	14.4	24.8
	Ts_wall	41.3	14	29.2		Ts_wall	34.8	15.2	24.3
L2.a	Ts_roof	40.5	9.7	25.7	L2.a	Ts_roof	34.2	11.4	21.6
	Ts_road	37.4	13.7	26.6		Ts_road	31.6	14.9	22.7
	Ts_wall	37.1	13.5	26.8		Ts_wall	31.2	14.9	22.8
L2.b	Ts_roof	40.3	9.4	25.6	L2.b	Ts_roof	34	11.5	21.5
	Ts_road	39	12.9	26.7		Ts_road	33.1	14.1	22.5
	Ts_wall	37.4	13.5	26.9		Ts_wall	31.5	15	22.8
L3.a	Ts_roof	40.5	9.7	25.7	L3.a	Ts_roof	34.2	11.4	21.6
	Ts_road	37.4	13.7	26.6		Ts_road	31.6	14.9	22.7
	Ts_wall	37.1	13.5	26.8		Ts_wall	31.2	14.9	22.8
L3.b	Ts_roof	40.3	9.4	25.6	L3.b	Ts_roof	34	11.5	21.5
	Ts_road	39	12.9	26.7		Ts_road	33.1	14.1	22.5
	Ts_wall	37.4	13.5	26.9		Ts_wall	31.5	15	22.8
H1.a	Ts_roof	70.5	10.3	35.3	H1.a	Ts_roof	61.1	12.4	26.9
	Ts_road	36.9	17.2	28.2		Ts_road	32	17.5	24.3
	Ts_wall	37.9	17.1	29		Ts_wall	31.4	17.6	24.5
H1.b	Ts_roof	70.5	10.3	35.3	H1.b	Ts_roof	61.1	12.4	26.9
	Ts_road	36.9	17.2	28.2		Ts_road	35	17.5	24.6
	Ts_wall	37.9	17.1	29		Ts_wall	31.4	17.6	24.5
H2.a	Ts_roof	42.6	10.3	27.1	H2.a	Ts_roof	36.8	12.4	22.6
	Ts_road	35.8	17.2	27.9		Ts_road	30.3	17.5	24.1
	Ts_wall	36.9	16.9	28.4		Ts_wall	30.7	17.5	24.3
H2.b	Ts_roof	42.5	10.3	27.1	H2.b	Ts_roof	36.8	12.4	22.6
	Ts_road	37	17.1	28.3		Ts_road	31.3	17.5	24.3
	Ts_wall	37	16.9	28.4		Ts_wall	30.7	17.5	24.3
H3.a	Ts_roof	42.6	10.3	27.1	H3.a	Ts_roof	36.8	12.4	22.6
	Ts_road	35.8	17.2	27.9		Ts_road	30.3	17.5	24.1
	Ts_wall	36.9	16.9	28.4		Ts_wall	30.7	17.5	24.3
H3.b	Ts_roof	42.5	10.3	27.1	H3.b	Ts_roof	36.8	12.4	22.6
	Ts_road	37	17.1	28.3		Ts_road	31.3	17.5	24.3
	Ts_wall	37	16.9	28.4		Ts_wall	30.7	17.5	24.3

Source: Elaborated by the author, 2019.

ated scenarios. Another determining factor is that in the physical model of UWG (Matlab code of UWG v.4.1), only the heat transfer phenomena (such as evap-

orative cooling) that they produce on the air is considered, not including the effect of the shadows that trees cast on the surfaces of facades and roofs.

## Discussion and conclusions

The UWG model is a very efficient tool in terms of runtime since it builds modified climate databases with geometric and morphological parameters of a referential city in shorter simulation processes compared to other urban simulators in the cities of Mendoza and Campinas. This was also demonstrated by Mao et al. (2018) who verified the limited natural time to accelerate calibration processes in the city of Abu Dhabi. However, it has been demonstrated that the UWG simulations produced mesoscale UHIs following the assumption that the air in the UCL was well-mixed. For these reasons, the integration of microscale UHIs and thermal comfort simulations is necessary to increase the reliability of the analysis' outcome as described in Kim et al. (2018).

As discuss Hong et al. (2020), computational tools empowered with rich urban data sets can model the performance of buildings at the urban scale to provide quantitative insights for decision makers on urban energy planning. These tools can also scale building energy retrofits at scale, to achieve efficiency, sustainability, and resilience of urban buildings. In this sense, the UWG model is versatile and compatible with building energy simulators such as the EnergyPlus because their databases have an \*.epw extension. As demonstrated by several authors, this information allows a greater veracity and adjustment of studies on a building's thermal behavior in an urban environment, as on the effect of the heat island in the construction of building energy consumption profiles (Palme & Salvati, 2018; Salvati et al., 2019; Sola et al., 2018). The UWG model has a great capacity to sensitively predict the results of the application of different mitigation strategies on the surface temperatures of the elements of the urban-building envelopes (walls, roofs and road). This is a useful knowledge to determine the degree of comfort of an urban space, as well as the possible energy savings in different climatic contexts. Due to the seasonal climatic rigor of the city of Mendoza, the modification in H/W and albedo recorded greater impact potential on surface temperatures than in Campinas. For example, when raising albedo levels in the enveloped of a scenario, surface temperatures of roofs decrease in up to 28 °C in Mendoza and 24.3 °C in Campinas (in Mendoza H1.a = 70.5 °C vs. H2.a / H3.a = 42.6 °C and in Campinas H1.a = 61.1 °C vs. H2.a / H3.a = 36.8 °C). This result evidences the great potential that the level of albedo produc-

es on the surface temperatures of the roof and consequently on the buildings' energy consumption. This result evidences the great potential that the level of albedo produces on the surface temperatures of the roof and consequently on the buildings' energy consumption.

Another strength detected in this work is that the UWG model can reflect the impact of anthropogenic heat flux derived from building densification, a parameter that most urban simulators do not consider in their energy budget calculations, but one which represents an important tool for urban guidelines. Although the veracity of anthropogenic heat predicted by the UWG model depends on the fitting of diverse inputs and considerations as discussed in Bueno et al. (2014), having this output is important in order to assess the impact over urban climate derived from the application of densification strategies on cities. Among the weaknesses detected, particularly in the scenarios analyzed in this work during the summer period, the UWG model showed a low sensitivity to the modification of air temperatures between urban overheating mitigation strategies. In addition, the UWG model is not sensitive to the modification of optical properties in walls because the scenarios with high albedo and combined albedo presented identical behavior, both in their air and surface temperatures. This conclusion is based on findings obtained in previous works carried out by Alchapar et al. (2017), in which it was sought to determine the thermal benefit of mitigation strategies of ICU over the city of Mendoza and Campinas through the use of ENVI-met software. The research with ENVI-met found differences in air temperature between scenarios of 3.5 °C for Mendoza and 5 °C in Campinas.

When modifying the vegetation parameters, the UWG model showed sensitivity ( $\Delta T_{s\_calle} = 5 \text{ °C}$ ) in road surface temperatures only in scenarios with low albedo and low H/W for both cities. This fact is explained because the calculation of the energy balance of the UWG model considers the vegetation and trees in a simplified way, assuming that a certain fraction of the absorbed solar radiation is transformed into latent heat and does not contribute to the increase of temperatures in the canyon (Mao et al., 2017). In addition, it assumes that trees are lower than buildings, so they do not participate in the calculation of surface temperature of roofs and facades. To avoid these short-

comings, the UWG model is constantly updated and developed, a process that results in a robust and operational software for predicting urban climatic conditions and for analyzing the interactions between buildings and their urban environment.

These findings are coincident with investigations of Bande et al. (2019) in Abu Dhabi, which showed that the UWG model tends to overestimate the canyon temperature during the summer and has a more realistic estimation in the winter season. Anyway, ENVI-met has better estimations of temperatures during the summer season compared to the UWG. The study also showed that the UWG weather file contrib-

utes a more detailed energy model and that ENVI-met needs improvement in calculating the anthropogenic heat and in calculation of the mean radiant temperature

Although this research is in an initial stage, the work showed that, in order to explain the behaviors of urban surfaces and the interactions with the climate, the use of climatic simulations with different scales of analysis is essential. That is why future works propose the use of the energy balance model -UWG- simultaneously with the microclimate model -ENVI-met- to enhance its capabilities.

## Acknowledgments

*This work was supported by the National Agency for Scientific and Technological Promotion-ANPCyT- of Argentina, through the Fund for Scientific and Technological Research -FONCyT (PICT2017-3248) and the State of São Paulo Research Foundation – FAPESP (2019/10308-9).*

## References

- Acero, J. A., & Herranz-Pascual, K. (2015). A comparison of thermal comfort conditions in four urban spaces by means of measurements and modelling techniques. *Building and Environment*, 93, 245–257. <https://doi.org/10.1016/j.buildenv.2015.06.028>
- Alchapar, Noelia L., & Correa, E. N. (2016). The use of reflective materials as a strategy for urban cooling in an arid “OASIS” city. *Sustainable Cities and Society*, 27, 1–14. <https://doi.org/10.1016/j.scs.2016.08.015>
- Alchapar, Noelia Liliana, Pezzuto, C. C., Correa, E. N., & Chebel Labaki, L. (2017). The impact of different cooling strategies on urban air temperatures: the cases of Campinas, Brazil and Mendoza, Argentina. *Theoretical and Applied Climatology*, 130(1–2), 35–50. <https://doi.org/10.1007/s00704-016-1851-5>
- Bande, L., Afshari, A., Masri, D. Al, Jha, M., Norford, L., Tsoupos, A., ... Armstrong, P. (2019). *Validation of UWG and ENVI-Met Models in an Abu Dhabi District, Based on Site Measurements*.
- Bowler, D. E., Buyung-Ali, L., Knight, T. M., & Pullin, A. S. (2010). Urban greening to cool towns and cities: A systematic review of the empirical evidence. *Landscape and Urban Planning*, 97(3), 147–155. <https://doi.org/10.1016/j.landurbplan.2010.05.006>
- Bruse, M., & Flerer, H. (1998). Simulating surface-plant-air interactions inside urban environments with a three dimensional numerical model. *Environmental Modelling & Software*, 13(3–4), 373–384.
- Bueno, B., Hidalgo, J., Pigeon, G., Norford, L., & Masson, V. (2013a). Calculation of air temperatures above the urban canopy layer from measurements at a rural operational weather station. *Journal of Applied Meteorology and Climatology*, 52(2), 472–483. <https://doi.org/10.1175/JAMC-D-12-083.1>
- Bueno, B., Nakano, A., & Norford, L. (2015). Urban weather generator: A method to predict neighborhood-specific urban temperatures for use in building energy simulations. *ICUC9 - 9th International Conference on Urban Climate Jointly with 12th Symposium on the Urban Environment*. Toulouse, France.
- Bueno, B., Norford, L., Hidalgo, J., & Pigeon, G. (2013b). The urban weather generator. *Journal of Building Performance Simulation*, 6(4), 269–281. <https://doi.org/10.1080/19401493.2012.718797>
- Bueno, B., Roth, M., Norford, L., & Li, R. (2014). Computationally efficient prediction of canopy level urban air temperature at the neighbourhood scale. *Urban Climate*, 9, 35–53. <https://doi.org/10.1016/j.uclim.2014.05.005>
- Chang, C. R., & Li, M. H. (2014). Effects of urban parks on the local urban thermal environment. *Urban Forestry and Urban Greening*, 13(4), 672–681. <https://doi.org/10.1016/j.ufug.2014.08.001>
- Climate.OneBuilding.Org. (2019). Repository of free climate data for building performance simulation. Retrieved July 1, 2019, from <http://climate.onebuilding.org/>
- Correa, E. N. (2006). *Isla de calor urbana. El caso del área metropolitana de Mendoza*. UNSA, Salta, Argentina.
- Doyon, B., Bélanger, D., & Gosselin, P. (2008). The potential impact of climate change on annual and sea-

- sonal mortality for three cities in Québec, Canada. *International Journal of Health Geographics*, 7, 1–12. <https://doi.org/10.1186/1476-072X-7-23>
- GOOGLE-EARTH. (2019). Mapa. Retrieved March 19, 2019, from <https://www.google.com.br/intl/pt-PT/earth/>
- Hong, T., Chen, Y., Luo, X., Luo, N., & Lee, S. H. (2020). Ten questions on urban building energy modeling. *Building and Environment*, 168(August 2019), 106508. <https://doi.org/10.1016/j.buildenv.2019.106508>
- Kim, H., Gu, D., & Kim, H. Y. (2018). Effects of Urban Heat Island mitigation in various climate zones in the United States. *Sustainable Cities and Society*, 41(June), 841–852. <https://doi.org/10.1016/j.scs.2018.06.021>
- Kotteck, M., Jurgen Grieser, Beck, C., Rudolf, B., & Rubel, F. (2006). World Map of the Köppen-Geiger climate classification updated. *Meteorologische Zeitschrift*, 3(3), 259–263. <https://doi.org/10.5194/hess-11-1633-2007>
- Mao, J., Fu, Y., Afshari, A., Armstrong, P. R., & Norford, L. K. (2018). Optimization-aided calibration of an urban microclimate model under uncertainty. *Building and Environment*, 143(April), 390–403. <https://doi.org/10.1016/j.buildenv.2018.07.034>
- Mao, J., Yang, J. H., Afshari, A., & Norford, L. K. (2017). Global sensitivity analysis of an urban microclimate system under uncertainty: Design and case study. *Building and Environment*, 124, 153–170. <https://doi.org/10.1016/j.buildenv.2017.08.011>
- Masson, V. (2000). A physically-based scheme for the urban energy budget in atmospheric models. *Boundary-Layer Meteorology*, 94(3), 357–397. <https://doi.org/10.1023/A:1002463829265>
- Mirzaei, P. A., & Haghighat, F. (2010). Approaches to study Urban Heat Island e Abilities and limitations. *Building and Environment*, 45(10), 2192–2201. <https://doi.org/10.1016/j.buildenv.2010.04.001>
- Ooka, R. (2007). Recent development of assessment tools for urban climate and heat-island investigation especially based on experiences in Japan. *Int. J. Climatol*, 27, 1919–1930. <https://doi.org/10.1002/joc>
- Palme, M., Inostroza, L., & Salvati, A. (2018). Technomass and cooling demand in South America: a superlinear relationship? *Building Research & Information*, 46(8), 864–880. <https://doi.org/10.1080/09613218.2018.1483868>
- Palme, M., Lobato, A., & Carrasco, C. (2016). Quantitative Analysis of Factors Contributing to Urban Heat Island Effect in Cities of Latin-American Pacific Coast. *Procedia Engineering*, 169(March 2019), 199–206. <https://doi.org/10.1016/j.proeng.2016.10.024>
- Palme, M., & Salvati, A. (2018). UWG -TRNSYS Simulation Coupling for Urban Building Energy Modelling. *4th Building Simulation and Optimization Conference*, (September). Cambridge, UK.
- Perini, K., & Magliocco, A. (2014). Urban Forestry & Urban Greening Effects of vegetation , urban density , building height , and atmospheric conditions on local temperatures and thermal comfort. *Urban Forestry & Urban Greening*, 13(3), 495–506. <https://doi.org/10.1016/j.ufug.2014.03.003>
- Pezzuto, C. C. (2007). *Avaliação do ambiente térmico nos espaços urbanos abertos. Estudo de caso em Campinas, SP*. Universidade Estadual de Campinas Faculdade.
- Salvati, A., Monti, P., Coch Roura, H., & Cecere, C. (2019). Climatic performance of urban textures: Analysis tools for a Mediterranean urban context. *Energy and Buildings*, 185, 162–179. <https://doi.org/10.1016/j.enbuild.2018.12.024>
- Salvati, A., Palme, M., & Inostroza, L. (2017). Key Parameters for Urban Heat Island Assessment in A Mediterranean Context: A Sensitivity Analysis Using the Urban Weather Generator Model. IOP Conference Series: Materials Science and Engineering, 245(8). <https://doi.org/10.1088/1757-899X/245/8/082055>
- Sola, A., Corchero, C., Salom, J., & Sanmarti, M. (2018). Simulation Tools to Build Urban-Scale Energy Models: A Review. *Energies*, 11(12), 3269. <https://doi.org/10.3390/en11123269>
- Sosa, M. B., Cantaloube, E. C., & Canton, M. A. (2017). Forma urbana y comportamiento térmico exterior. Un estudio para reducir la isla de calor urbana en una ciudad árida . Urban form and outdoor thermal behavior . A study for reduce the urban heat island in an arid city . *Estudios Del Habitat*, 15(2), 1–12.
- Yang, X., Zhao, L., Bruse, M., & Meng, Q. (2013). Evaluation of a microclimate model for predicting the thermal behavior of different ground surfaces. *Building and Environment*, 60, 93–104. <https://doi.org/10.1016/j.buildenv.2012.11.008>